

## DEVELOPMENT OF A COMPACT MERCURY TARGET WITH BUBBLING EQUIPMENT TO MITIGATE PRESSURE WAVES

Katsuhiro HAGA, Takashi WAKUI, Kokei HANANO, Hiroyuki KOGAWA,  
Takashi NAOE, Masato IDA, Masatoshi FUTAKAWA  
*Neutron Source Section, J-PARC Center, Japan Atomic Energy Agency  
2-4 Shirakata-Shirane, Tokai-mura, Naka-gun, Ibaraki  
319-1195, JAPAN*

### ABSTRACT

A mercury target has been installed at the Materials and Life science experimental Facility (MLF) in the Japan Proton Accelerator Research Complex (J-PARC). The modification of the target structure is being required from the viewpoints of fabrication cost, wastage storage, and the prevention of a seal flange fixed at target trolley from contact damage. The present target vessel, 2 m in length, will be compactly separated into the fore and rear parts, a so-called compact target vessel. The fore part of ca.1 m in length will be periodically replaced due to heavy irradiation damage and the rear part has two connecting flanges at each end to connect with the fore part and with a permanent seal structure fixed at the target trolley. The bubbling equipment will be installed in the fore part to mitigate the pressure waves induced by pulsed high intensity proton beam injection into mercury. The design and the required R&D associated with the compact target will be shown in this paper.

### 1. Introduction

A mercury target is running as the spallation neutron source at the Materials and Life science experimental Facility (MLF) in the Japan Proton Accelerator Research Complex (J-PARC) [1]. The size of the present target is 2.3 m in length and 1 m in height and width, which will be called the full size target in this paper [2]. After two years operation since the first proton beam was injected to the mercury target, a new target is going to be fabricated as a spare target, and the modification of the target structure is crucially required from the viewpoints of wastage storage, fabrication cost, and the prevention of a seal flange fixed at target trolley from contact damage. The structure of the new target is like that the full size target is separated into the fore and rear parts as shown in Fig. 1, which will be called a compact target. The fore part, which is ca.1 m in length, will suffer from heavy irradiation damage and will be replaced periodically. On the other hand, the rear part will be used for a long time. The fore part is connected to the rear part by bolts at the additional flange, which is one of the key components for the successful design of the

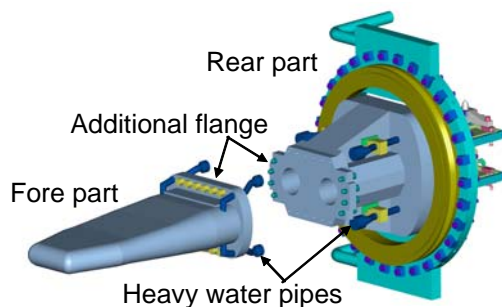


Fig. 1 Schematic view of the compact target

**ICANS XIX,**  
**19th meeting on Collaboration of Advanced Neutron Sources**  
March 8 – 12, 2010  
Grindelwald, Switzerland

compact target. Four pipes installed around the additional flange are heavy water lines to cool the outer shroud of the target vessel. The bubbling equipment will be installed in the fore part to mitigate the pressure waves induced by pulsed high intensity proton beam injection into mercury.

In this paper, the design and the results of R&D associated with the compact target will be shown, including design of the additional flange, the results of the seal flange mock-up tests, the remote handling scenario, and bubble distribution in the compact target.

## **2. Merits and concerns**

The compact target has several important merits. Firstly, the volume of the radioactive waste, i.e. the used target vessel, can be drastically reduced to almost 1/8 of the full size target. The lifetime of the target vessel is assumed to be half a year at 1 MW beam power operation, and more than 60 used target vessels will become the highly radioactive wastes during the lifetime of the facility. Because the storage place for the radioactive waste is limited, reduction of the waste volume has a great merit to improve the space utility and to prolong the storage period before they will be transported to the back-end facility. This will enable us to have enough time to reduce the radiation level of the used target, which will require less shielding of the transportation cask. Secondly, the seal plane of the permanent flange of mercury pipe, which is mounted on the rear side of the target vessel, can be protected by adding the additional flange between the fore part and rear part of the compact target. The possibility that the permanent flange will be damaged can be reduced by reducing the frequency of access to the permanent flange. Thirdly, the cost to fabricate the fore part, which is replaced frequently, can be reduced to ca. 40 % of the full size target.

Though the compact target has such attractive merits, there are some concerns that have to be investigated. Firstly, the additional flange must have excellent seal performance against mercury and helium. This concern was checked and demonstrated by the mockup tests. Secondly, the fore part of the compact target must be replaced smoothly just like the full size target by remote handling operation. Interference with the remote handling tools was checked by three dimensional CAD, and also checked using the mockup model. The results of R&D for these concerns will be mentioned later in detail.

## **3. Design of the additional flange**

### *3.1 Overview*

The schematic drawing of the additional flange is shown in Fig. 2. There are two mercury lines and helium gas lines for the bubbling in the additional flange. The helium gas lines in the space between double knife edges are used for monitoring the mercury leakage. Mercury leakage through an inner knife edge can be detected immediately before the leakage penetrates the outer knife edge. Sensor cables of 5 thermocouples and 2 sets of mercury detectors are integrated into one connector and mounted on the additional flange. Two positioning pins are also mounted, which is used to adjust the connecting positions of the flanges. Under the mercury lines, there is a tray to catch the mercury drop during the target exchange process. The volume ca. 30 cm<sup>3</sup> of the tray is larger enough to catch the estimated mercury drop of 2 cm<sup>3</sup>.

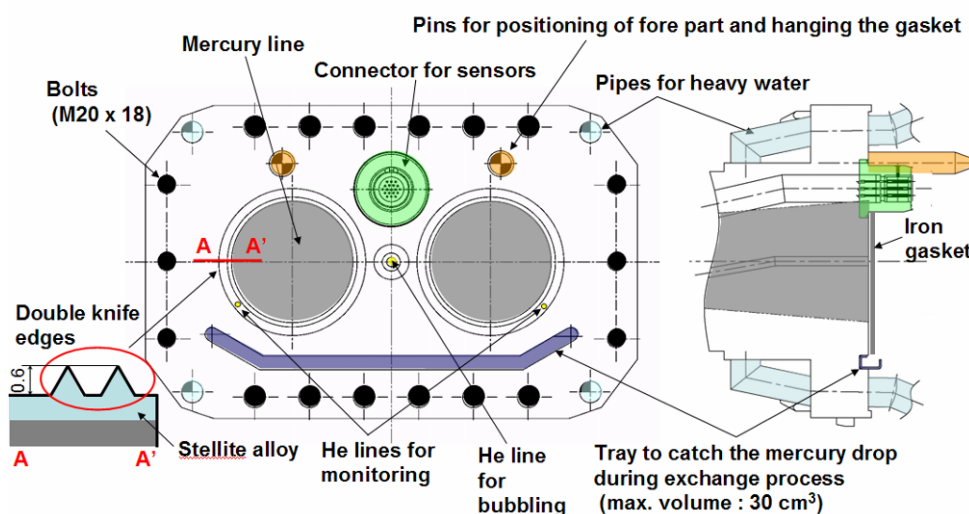


Fig. 2 Schematic drawing of the additional flange

### 3.2 Endurance of the knife edges

A double knife edge was adopted to seal the mercury and helium gas lines. The material of the knife edge is Stellite alloy that is about four times as hard as an iron gasket. The shape of the knife edge is an equilateral triangle with a nominal height of 0.6 mm. In order to confirm the endurance of the knife edge, indentation tests were carried out using a small piece of knife edge model. The knife edge of the model was pushed onto an iron gasket to the depth of 0.3 mm many times and the deformation of the knife edge was measured. After 200 times of indentation, the deformation of knife edge was only 5  $\mu\text{m}$  in height and enough endurance was confirmed.

### 3.3 Depth of indentation on the gasket

Because the additional flange seals two mercury lines and one helium gas line all together using the combination of knife edges and iron gasket, we assumed that the seal performance of the additional flange would be affected by several factors which are (1) Uniformity of height of knife edges, (2) Deflection of the flange, (3) Fastening procedure of the bolts. The seal performance is secured by close contact between the knife edge and the iron gasket, and the indentation depth can be the barometer of closeness of the contact. Thus, we estimated the indentation depth needed to absorb the tolerances of each factors shown above. The criterion of minimum indentation depth was set 0.1 mm based on the results of seal performance tests carried out in the past for the present target. Tolerance of 0.1 mm was given to factor (1) taking the empirical estimation into consideration. Another tolerance of 0.1 mm was given to factor (2). No tolerance was given to factor (3), because it is not the property of the flange itself. Thus, the total indentation depth that has to be fulfilled was 0.3 mm, and the additional flange was designed to fulfill this condition.

The number of bolts necessary to indent 0.3 mm on average was estimated. The bolt size, the fastening torque and total length of knife edge were M20, 200 N m and 2.2 m, respectively. The estimated minimum number of bolts was 12. Taking into account a scatter of the fastening force when all bolts were fastened by remote handling, the number of bolts was increased by 1.5 times to 18. The thicknesses of the flange of the fore and rear parts were designed to be 70 and 50 mm respectively to minimize the flange deflection, while taking the interface integrity between the compact target and the surrounding components into consideration.

In order to estimate the indentation depth and the deformation of the flange, a numerical analysis was carried out using quarter model of the flange part as shown in

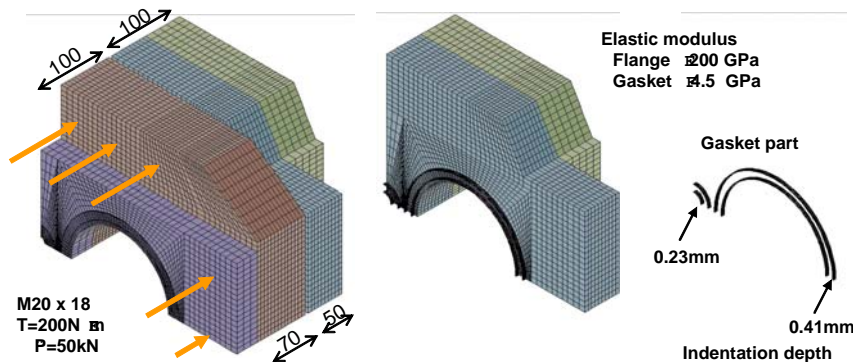


Fig. 3 Analytical model for the additional flange

Fig.3. The results showed that maximum and minimum indentation depths were 0.41 and 0.23 mm respectively. The difference of these two values 0.17 mm corresponds to the flange deflection. Though it was larger than the assumed value of 0.1 mm, the minimum indentation depth of 0.23 mm still fulfilled the minimum criterion of 0.1 mm, even if the tolerance due to factor (1) was taken into consideration

### 3.4 Mockup tests of the additional flange

In order to confirm the seal performance at an additional flange, a mockup model was fabricated as shown in Fig. 4. The test results will be mentioned in this chapter.

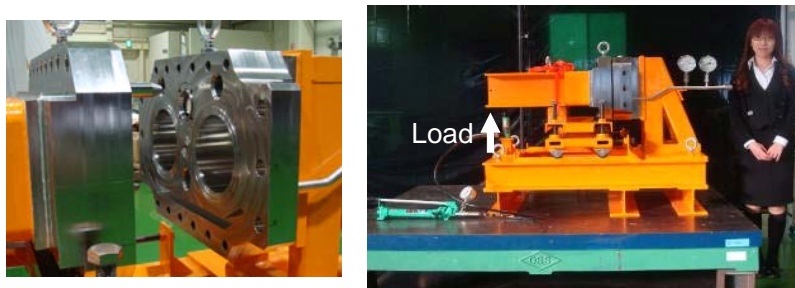


Fig. 4 A mockup model of the additional flange

#### (1) Uniformity of height of knife edges

Height of all the knife edges on a flange plane should be uniform for the good seal performance, and it depends on the accuracy of machining technique. Because the stellite alloy was welded on the flange to form knife edges, there was a possibility of deformation of flange due to the release of residual stress while the knife edges were machined by a lathe and the uniformity of the knife edge height might be degraded. Figure 5 shows the

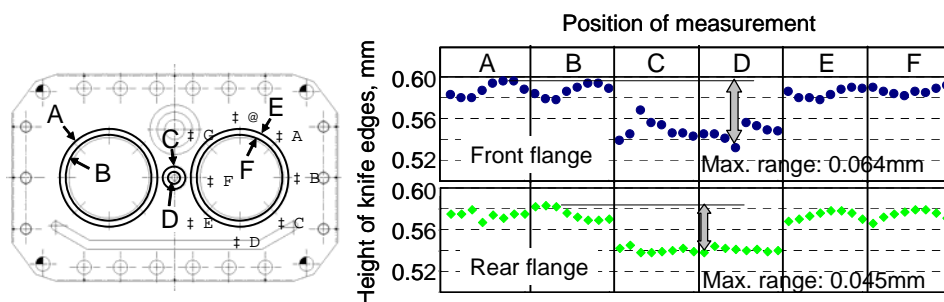


Fig. 5 Distribution of the knife edge height

distribution of knife edge height of the mockup model. It can be seen that the maximum range of height was 0.064 mm in the front flange and 0.045 mm in the rear flange, which shows that the height of knife edges were made within the tolerance of 0.1 mm. Because the tolerance was fulfilled in both the two flanges, the reproducibility of machining is considered to be good and, furthermore, the machining accuracy will be improved in the actual target.

(2) Deflection of the flange

After the bolts of the mockup model were fastened with rated torque, the deflection of the flange along the vertical axis was measured as shown in Fig. 6. The gap between the straight ruler and the flange surface was 0.1 mm, which was well below the estimation of 0.17 mm. Because the flange will be thicker in the actual target vessel, the deflection will become smaller.

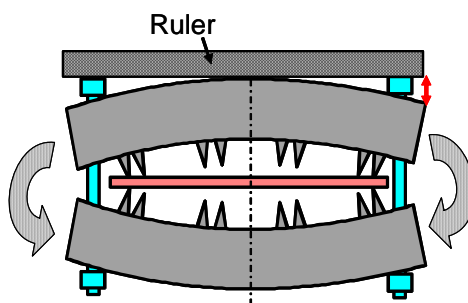


Fig. 6 Measurement of the flange deflection

(3) Fastening procedure of the bolts

18 bolts on the additional flange were fastened in accordance with the remote handling procedure, in which the bolts are divided into several groups and fastened sequentially from one group to next group. The torque for fastening bolts took discrete values such as 60 N.m, 120 N.m and 200 N.m. The indentation depth and the seal performance were compared with the case in which the bolts were fastened carefully by hands-on operation. Figure 7 shows distribution of the indentation depth on the iron gasket, which contains the effect of all factors from (1) to (3). The indentation depth was shallower at the center knife edge, which was caused by the low height of knife edges and the flange deflection, but it still fulfilled the criterion of minimum depth of 0.1 mm. Decrease of the indentation depth by the remote handling procedure was observed, but it can be improved by optimizing the sequence of fastening the bolts.

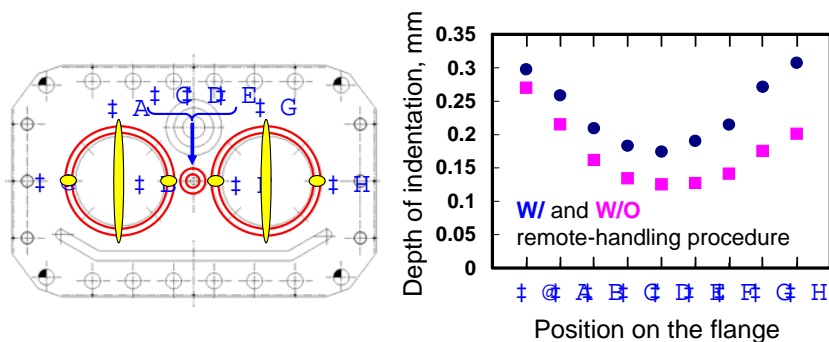


Fig. 7 Distribution of indentation depth on the gasket

### 3.5 Seal performance tests

Seal performance tests of the additional flange were carried out using mock up model. Mercury lines and helium gas line for bubbling were pressurized up to 0.5 MPa and the helium leak rates were measured. Bending moment was applied to the mockup model using an oil jack to simulate the dead weight of mercury and seismic load as shown in Fig. 4. The test was carried out both for the cases of with and without the remote handling procedure of fastening the bolts.

Figure 8 shows the results. The helium leak rate was less than the order of  $10^{-9}$  Pa.m<sup>3</sup>/s and fulfilled the criterion of  $10^{-6}$  Pa.m<sup>3</sup>/s in all the cases. There were no influences observed by the bending moment or the remote handling procedure, which implied the robustness of the seal performance of the additional flange.

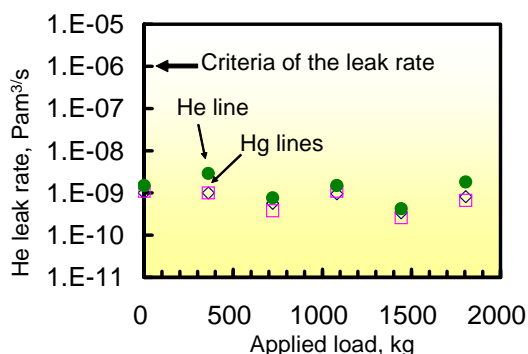


Fig. 8 Results of the seal performance test

## 4. Remote handling of the target vessel

A fore part of the compact mercury target can be exchanged in almost the same way with the full size target. Figure 9 shows the remote handling procedure to remove the fore part. The operation period to replace the fore part of the compact target is about three days, which is two days shorter than that to replace the full size target. The interference between the components and the remote handling procedure were checked by the simulations using 3D CAD. A mockup model that simulates the position of bolts on the additional flange

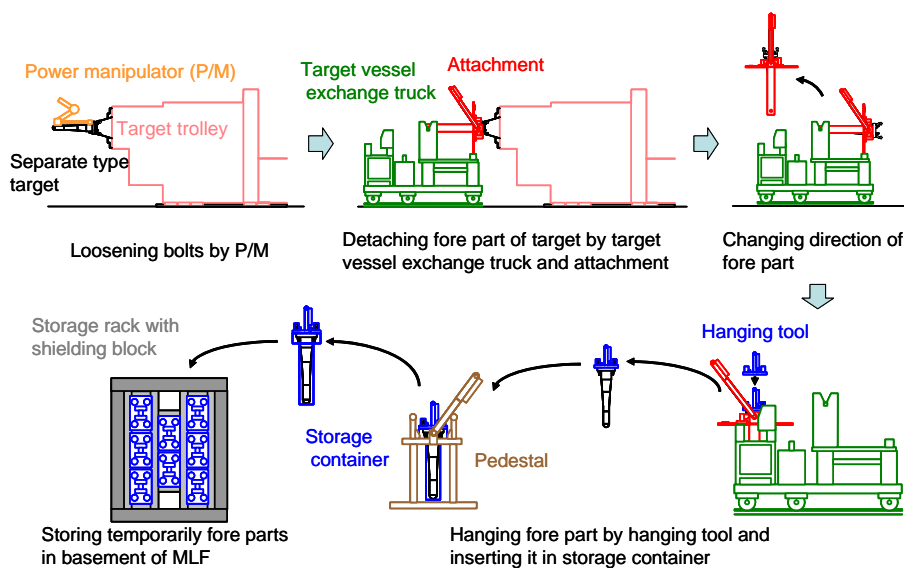


Fig. 9 Remote handling procedure to exchange the target

was also fabricated and the interference with the operation tool was checked using the actual target system. Positioning data of the operation tool was taken in advance using the mockup model.

## 5. Installation of a bubbler

Injection of pulsed high power proton beam causes pressure wave in mercury and the pressure wave induces cavitation and damages the mercury vessel wall. In order to mitigate the pressure waves in mercury, a helium bubble injector will be installed in the mercury target. The effect of the mitigation depends on a bubble size and a void fraction, but there was a possibility that the strong buoyancy of bubbles in mercury prevents bubbles from reaching the desirable place. Thus, the bubble distribution in the target vessel was evaluated using the computational simulation. The commercial base thermal hydraulic code, FLUENT, was used for the simulations. The helium bubble flow in the mercury flow field was simulated using a DPM (Discrete Phase Model). With DPM the helium bubbles are treated as tiny spherical particles, and the interaction between particles are ignored under the precondition that the bubble void fraction is very small, which is less than several percent.

Figure 10(a) shows the mercury velocity field and the flow vane arrangement. The mercury flow rate was  $41 \text{ m}^3/\text{hr}$ , which is the rated flow rate of the actual target system, and the volume ratio of the injected helium gas to mercury was 0.1 %. The bubble injector was installed at the inlet of the target vessel. As shown in Fig. 10(b), large amount of bubbles with the diameter of  $200 \text{ }\mu\text{m}$  could reach the beam window without rising up to the top wall, but there are still some concerns such as the influence of bubble coalescences and degradation of the cooling performance by bubbles. We are investigating them by analyses and experiments using mock up models.

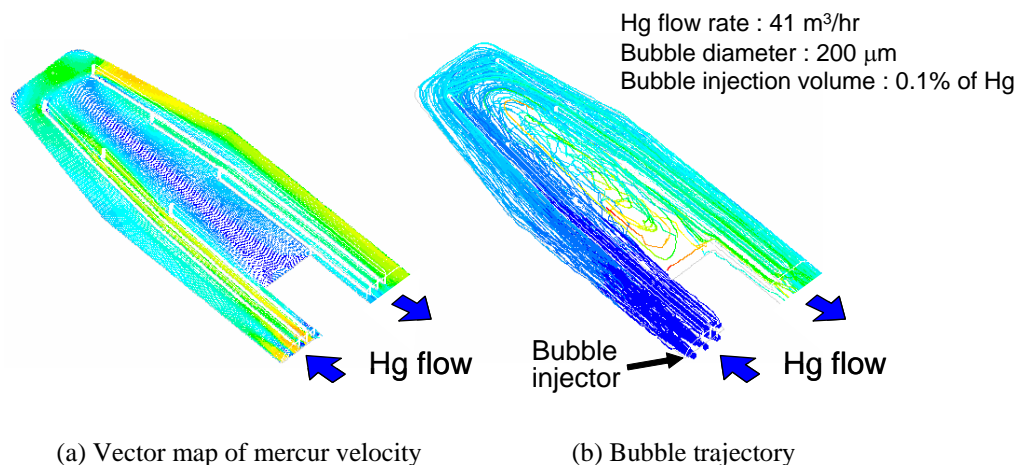


Fig. 10 Simulation results of the bubble flow in the target

## 6. Summary

The design of the compact target and remote handling procedure has been almost completed. The ordering procedure of the compact target has been already started and detail design will be carried out with manufacturer. The design of the bubbling equipment will be also promoted further.

**ICANS XIX,**  
**19th meeting on Collaboration of Advanced Neutron Sources**  
March 8 – 12, 2010  
Grindelwald, Switzerland

The compact target vessel with bubbling equipment is scheduled to be installed during the system shutdown period in the summer 2011.

## **7. References**

1. S. Nagamiya, *Nuclear Physics A*, 774, (2006) p.895-898.
2. K. Haga et.al, *Proc. of ICONE12*, ICONE12-49518 (2004)